magnitude for the proton cross section at 70 Mev. Qualitatively, the "deuteron model" offers a nice explanation of the experimental indication that the proton receives about half the primary photon energy and of the forward assymmetry in the angular distribution. However, as can be seen in Figs. 6 and 9, the quantitative fit with the data is not good. On the other hand, the "one-nucleon model" fails, even qualitatively, to predict a "cutoff" in the energy spectrum but does give quite a reasonable fit to the data up to the "cutoff." (See Fig. 9.) In computing cross sections for their "one-nucleon model" Levinthal and Silverman used the nuclear momentum distribution given by Chew and Goldberger.[13] It is possible that this distribution incorporated into the "deuteron model" would give results in reasonable agreement with the experiments.

Processes involving mesonic interactions have been proposed as the explanation of photonuclear stars by Kikuchi[4] and Miller.[5] Some, and possibly all, of the protons observed in the present experiment must be prongs of these stars. While it is somewhat difficult to explain the angular distribution and the excitation function of the protons with meson models, the possibility that the protons may, at least in part, be associated with mesonic processes cannot be ruled out.‡

The author wishes to express his appreciation to Professor R. R. Wilson for his personal direction of this work. He is greatly indebted to Professor H. A. Bethe and to Doctors A. Silverman, J. S. Levinger, D. Walker, and S. Kikuchi for helpful discussions and communication of results. The assistance and cooperation of the many students and staff members who operated the synchrotron are gratefully acknowledged.

[13] G. F. Chew and M. L. Goldberger, Phys. Rev. **77**, 470 (1950).

‡ It has been suggested by R. R. Wilson that the process of proton production may involve the production and subsequent reabsorption of a meson in a deuteron-like subunit inside the nucleus. In this process momentum and energy are conserved between the incident photon and the emitted proton and neutron. Such a process could give results similar to those of Levinger's deuteron model and provide a qualitatively satisfactory explanation of the observations.

PHYSICAL REVIEW VOLUME 85, NUMBER 3 FEBRUARY 1, 1952

Proton-Proton Scattering at 240 Mev*

C. L. Oxley and R. D. Schamberger†
University of Rochester, Rochester, New York

(Received October 10, 1951)

Differential proton-proton scattering cross sections have been measured at six angles in the range from 27 to 90 degrees center of mass. The internal undeflected cyclotron beam was used with a hydrocarbon target. Proton-proton scattering was differentiated by detecting the emitted proton pair with its definite angle between particles in coincidence with two scintillation counters. Scintillator dimensions determined the solid angle accepted. The incident beam was monitored by measurement of the beta-activity induced by the reaction $C^{12}(p,pn)C^{11}$ in the target. General cyclotron background was negligible.

The cross sections measured show isotropy in the center-of-mass system within estimated errors. The average value of the cross section was 4.97 ± 0.43 millibarns/steradian based on a 49 ± 3 millibarn carbon cross section. This is in poor agreement with previous measurements of 3.6 ± 0.3 mb/steradian.

INTRODUCTION

THIS article describes an experimental method for measuring proton-proton scattering using the internal beam of the Rochester synchrocyclotron and presents experimental results obtained with 240-Mev protons. Preliminary reports of this work have been presented.[1] Differential cross sections have been measured at six angles in the range from 27 to 90 degrees, center of mass, obtaining an angular distribution and an absolute measure of the differential cross section.

Other proton-proton scattering results have been reported in the high energy range by Chamberlain, Segrè, and Wiegand,[2] who have made extensive measurements at 345 Mev and measurements at several angles at 249, 164, and 119 Mev. Birge, Kruse, and Ramsey,[3] using a method similar to that described here, reported measurements at 105 and 75 Mev. All measurements have shown the same general results: a center-of-mass cross section virtually independent of angle and energy.

APPARATUS AND PROCEDURE

General Description

The single dee construction of the cyclotron provided space within the tank for experimental equipment. A solid hydrocarbon target was used and the proton-proton scattering was differentiated by the method of Wilson and Creutz[4] in which counters in coincidence record the recoil and incident proton pair which

* This work has been supported by the ONR and AEC.

† Now at Brookhaven National Laboratory, Upton, New York.

[1] C. L. Oxley, Phys. Rev. **76**, 461 (1949); Oxley, Schamberger, and Towler, Phys. Rev. **82**, 295 (1951).

[2] O. Chamberlain and C. Wiegand, Phys. Rev. **79**, 81 (1950); Chamberlain, Segrè, and Wiegand, Phys. Rev. **81**, 2841 (1951); Phys. Rev. **83**, 923 (1951).

[3] Birge, Kruse, and Ramsey, Phys. Rev. **83**, 274 (1951).

[4] R. R. Wilson and E. C. Creutz, Phys. Rev. **71**, 339 (1947).

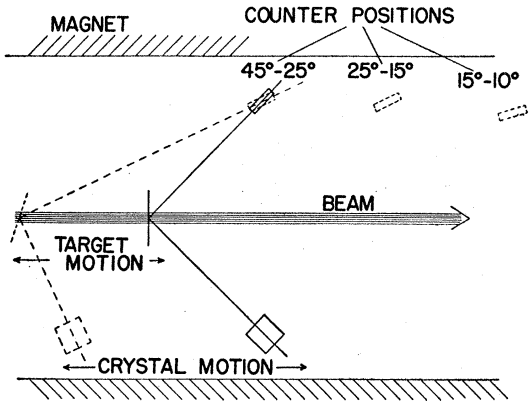

FIG. 1. Schematic section of experimental arrangement.

emerges from p-p scattering with a definite angle of approximately 90 degrees[5] between them. The counters used were anthracene scintillation type in which the anthracene dimensions served to define the effective area of the counter. Since the expansion of the beam per revolution is small, the use of a Faraday cage proton collector was impractical. Instead, the C^{11} beta-activity induced in the polyethylene target by the reaction $C^{12}(p,pn)C^{11}$ was measured. From the cross section for this reaction as measured by Aamodt, Peterson, and Phillips,[6] the incident number of protons could be calculated. Since the same number of protons passed the carbon and hydrogen of the target, the differential cross section was determined from the equation

$$\sigma_{pp}=N_p(\Theta)N_C\sigma_C/N_{C^{11}}N_H\Delta\Omega(\Theta),$$

where $N_p(\Theta)$ is the number of coincidences observed, $N_{C^{11}}$ is the number of C^{11} nuclei produced, N_C/N_H is the carbon to hydrogen ratio in the target material, σ_C is the cross section for the $C^{12}(p,pn)C^{11}$ process, and $\Delta\Omega(\Theta)$ is the solid angle subtended by the counters.

Figure 1 is a schematic section of the apparatus in the vertical plane tangent to the outer cyclotron orbit. The expanding beam struck the target, as indicated. The upper counter occupied a fixed position for the measurement of scattering in the range from 45 to 25 degrees (laboratory). The counters in all cases were well outside the dee gap near the magnet faces. The target and lower counter were movable continuously over the ranges indicated in the figure. The two extreme positions indicate, respectively, the settings at 45 and 25 degrees. For intermediate angles intermediate positions were set up by placing the lower counter in a calculated position and then moving the target until the number of coincidences observed indicated the proper target position. Two other positions were available for the upper counter, as indicated. With them, the range of scattering angles from 45 to 12 degrees was available. The target was tilted to reduce the energy loss of the large angle protons. In order to prevent excessive energy loss and multiple scattering of the lower energy scattered proton, the target thicknesses ranged from 12 to 72 mg/cm^2 according to scattering angle. Each target was made of 12 mg/cm^2 polyethylene laminations, so that β-counting could be carried out with a standard thickness of material.

Figure 2 is a photograph of the scattering apparatus. The apparatus was mounted on a port plate of the cyclotron vacuum chamber. The target was mounted at the end of a rod which passed through a Wilson seal, so that motion could be provided both radially and tangential to the proton orbits. These motions were

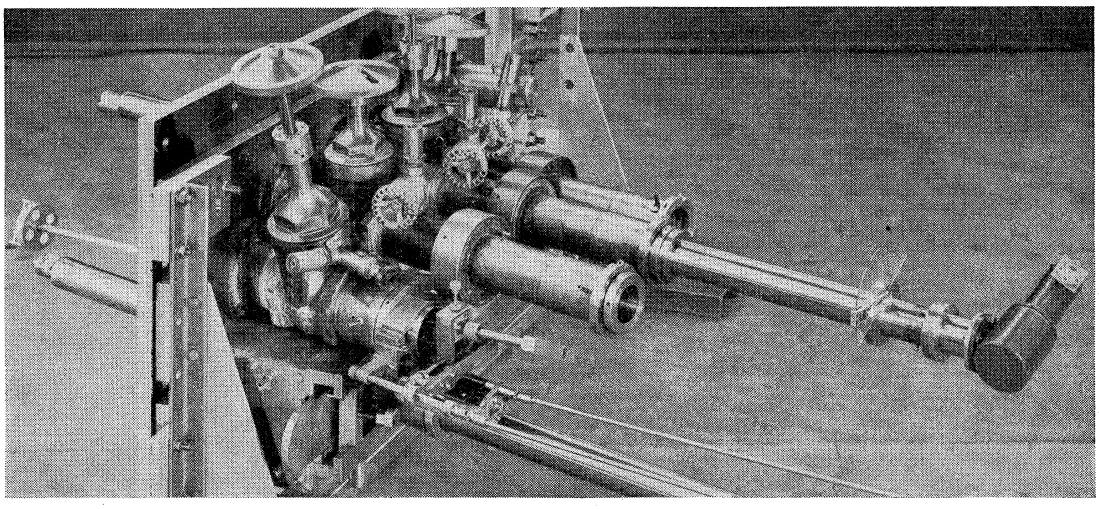

FIG. 2. Photograph of scattering apparatus on cyclotron port plate.

[5] The laboratory scattering angles Θ_1, and Θ_2 are given in terms of the c.m. angle θ by $\tan\Theta_1=(1-\beta'^2)^{\frac{1}{2}}\tan(\theta/2)$ and $\tan\Theta_2=(1-\beta'^2)^{\frac{1}{2}}\,\mathrm{ctn}(\theta/2)$ where β' is for the center of mass.

[6] Aamodt, Peterson, and Phillips, University of California Radiation Laboratory Report 526 (1949). We wish to thank Professor Panofsky and Dr. Aamodt for the loan of their secondary RaE standard source.

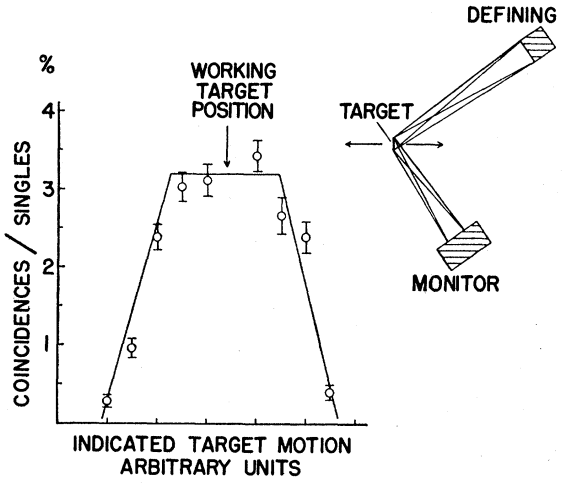

FIG. 3. Solid angle definition in vertical plane tangent to cyclotron orbit.

provided by remotely controlled selsyn motors which drove a carriage attached to the outside of the target rod. Shown also is one of the counter assemblies, which consisted of a 115-cm long stainless steel tube, at one end of which was the scintillator housing and at the other the magnetically shielded photomultiplier tube and preamplifier. A 2-cm diameter methacrylate plastic light pipe inside the tube connected phosphor and phototube. The steel tube passed into the cyclotron vacuum through a chevron seal, thus permitting rotation and radial adjustment. Gate valve locks were also provided for insertion of the counter tubes. The position of the lower counter assembly could be adjusted continuously in the direction tangent to the beam. The large vacuum box lock which permitted this adjustment is shown.

Solid Angle Definition

The method by which the counter geometry defined the solid angle for p-p coincidences is indicated in Figs. 3 and 4. For simplification, effects of the magnetic field are neglected here. Also shown in the figures is the effect of target motion on the coincidences. Figure 3 shows the view in the tangent plane as did Fig. 1. Here it is seen that one counter selected the p-p protons accepted in coincidence, while the other, the monitor counter, accepted a considerably larger angular spread than was necessary to receive the conjugate proton. Definition by one counter made the position of the target uncritical. The graph in Fig. 3 indicates the variation of the coincidences as a function of target position. The plateau was obtained as the p-p protons defined by one counter swept across the monitor counter. The singles rates in one counter were used here for normalization to constant beam. The backgrounds have been subtracted. Such data was collected and plotted for each scattering angle to determine the proper target position and to check on normal functioning of the apparatus.

In the vertical radial plane, a similar definition was involved, as is indicated in Fig. 4, but here we are perpendicular to the plane of scattering and the defining and monitor roles of the two counters have been reversed. Again radial motion produced coincidences over a range where one counter defined and the plateau was observed. The reversal of the defining and monitor roles in the two planes allowed use of a more readily available size of crystal. The target was placed at the midpoint of the plateau. The character of these plateaus gave assurance that the response of the crystals was essentially constant over their entire length.

In order to have precise knowledge of the solid angle defined by the counters, it was important to know the effect of incomplete collimation of protons from the target and of possible misalignment of the counter sides with the path of the protons the counters receive. These effects may be examined by reference to the pulse-height distribution in an ideal scintillator where the protons are presumed to pass completely through the counter and produce pulses proportional to the length of path in the crystal.

Figure 5 shows the case of protons proceeding at a small angle α with the scintillator sides. It may be seen that protons passing through the width W_f produce full pulse height; those passing through $W_{\frac{1}{2}}$ produce pulse heights of $\frac{1}{2}$ full height or higher; and those through W_0 produce pulses of height greater than 0. For small angles α, it may also be noted that $W_{\frac{1}{2}}$ is closely equal to the geometrical width of the crystal, differing only by a factor $\cos\alpha$. From these considerations, it is seen that the integral number-pulse height curve for the counter will fall slightly and linearly from zero pulse height to the pulse height corresponding to full passage through the crystal, where the number falls abruptly to zero. The fractional drop in number over the slowly falling part of the curve is proportional to α and amounts to approximately 5 percent per degree for the crystal dimensions used in the experiment. The same type of discriminator curve will be produced by incomplete collimation as by misalignment. In either case, however,

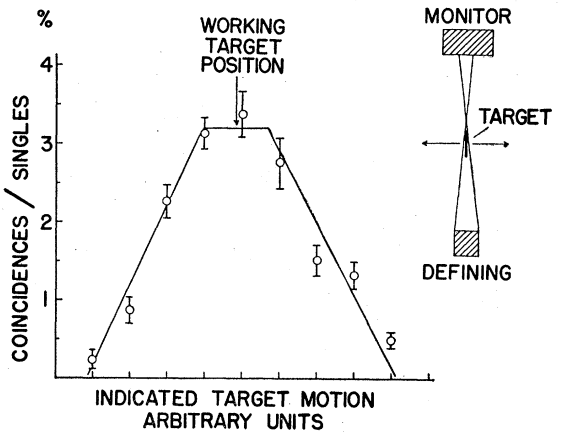

FIG. 4. Solid angle definition in radial vertical plane.

the setting of the discriminator level at a pulse height of half that for full passage through the crystal makes the effective width of the crystal very closely the geometrical width of the scintillator.

Figure 6 shows an experimentally measured integral number-discriminator curve, showing the general behavior predicted above. Two effects distorted the predictions of the ideal analysis. The first occurred because, for a definite length of proton path, there was a variation in pulse heights because of the different optical efficiencies in different parts of the crystal and to the statistical nature of the quantum and photoelectron emission. If the resulting distribution in pulse heights is symmetrical and not unduly broad, the pulse-height setting specified still gives an effective width closely equal to the geometrical width of the counter. Secondly, the specific ionization, and therefore, the number of photons produced was not constant. As a result, the discriminator had to be set at less than half of full pulse height to produce a selection corresponding to travel through half or more of the crystal.

In practice, the apparatus was adjusted with counters aligned according to calculation. Observation of number-pulse-height data as in Fig. 6, showing a curve with a small initial slope, indicated that the cross fire and misalignment effects were small, so that setting the discriminator at the level for passage through half the counter gave an effective counter width equal to the geometrical one.

The effects of the magnetic field in distorting the scattered proton paths were not large, but were considered. The proton paths were calculated and the target and counter positions so adjusted along the cyclotron radius that the proton entered the lower counter parallel to its defining sides. For the upper counter, the calculated paths showed that a tilt of the counter of 16 degrees from the radial would allow nearly parallel entry regardless of scattering angle. However, a more crucial adjustment was that made by the rotation of the upper counter around its radial axis, since this affected the solid angle definition directly. The angle of rotation was calculated for each scattering angle.

In addition to these effects of the magnetic field on the counter position and alignment, there were effects on the solid angle due to changes in trajectory and focusing action. Calculation of the solid angle becomes fairly complex. Details of the solid angle and path calculations are available from the authors.

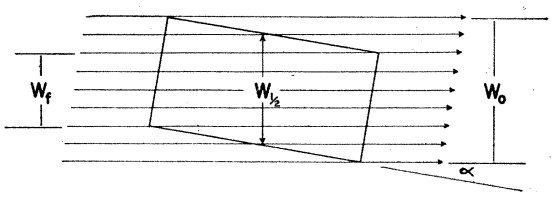

FIG. 5. Paths in misaligned scintillator.

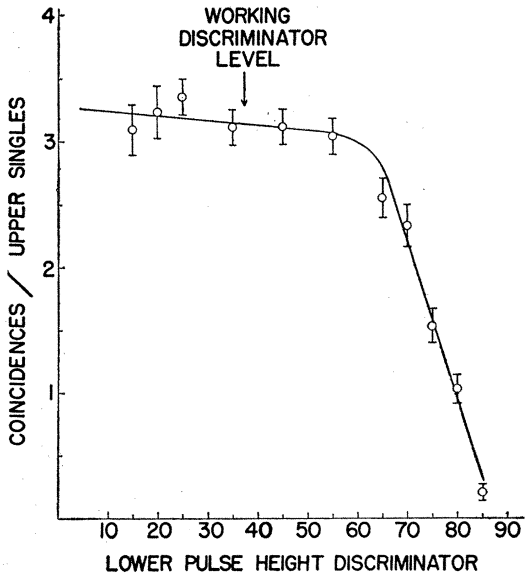

FIG. 6. Typical integral number-bias data.

Coincidence counts could be lost as a result of scattering and nuclear processes in the anthracene scintillators. The crystals were so mounted and used that three sides of the normally active volumes were bounded either by inactive anthracene or plastic of approximately the same density and composition. On these sides, scattering out of the active volume was well compensated by scattering in. The loss from the free side due to multiple Coulomb scattering has been estimated to have been approximately 0.5 percent at all angles. Nuclear processes may occur in as many as 5 percent of the traversals, but it has been estimated on the basis of proton star data[7] that this results in less than 1 percent loss of coincidences. No correction has been made for these losses.

Counters

The anthracene crystals, prepared by Mr. McGuire of this laboratory, were of excellent clarity with very few faults; good sensitivity was indicated from all parts of the crystal. They were cemented to the light pipe with Canada balsam and were provided with an aluminum foil reflector. The upper crystal, which received protons of 120 Mev or more, was in air within a 1-mm thick brass housing. The lower energy protons entered the lower crystal through a 4 mg/cm^2 aluminum foil used to provide light tightness. A vacuum seal was provided on a chromium coated part of the light pipe, so that this crystal was in the cyclotron vacuum, and the aluminum foil did not need to support air pressure. One pair of crystals was used throughout the experiment. The upper crystal was $1.98\times0.463\times2.65$ cm and the lower one, $2.00\times0.547\times1.40$ cm (dimensions in order of length to protons, defining dimension, remain-

[7] A. M. Perry (private communication).

ing dimension). Considering the crystal dimensions and the beam height of 1 cm an angular resolution of ± 3.5 degrees, c.m., is found for 90-degree scattering and ± 1.5 degrees, c.m., for 27 degrees.

Electronics

Two channels were provided in which the photomultiplier output of a few tenths of a volt passed to a cathode follower, which fed 300 feet of coaxial line leading to the control and laboratory building. There, each signal went directly to the input of a model 204 C Atomic Instruments Company linear amplifier (an adaptation of the Bell and Jordan amplier[8]) with its associated pulse-height discriminator. The discriminator output fed scalers and a coincidence circuit with a resolving time of about 3×10^{-7} sec. An oscilloscope, Dumont 248-A, was available for observation of single pulses in adjustment and check work.

Cyclotron Beam Characteristics

Two characteristics of the cyclotron operation are worthy of particular attention: the energy spectrum and the time structure of the beam pulses.

The synchronous orbit energy of the protons at the target radius, 148.5 cm ($n=0.2$), was calculated from the magnet current and field measurements to be 243 Mev. Measurement of the range of protons in copper after they had been scattered at small angles from a copper target at this radius indicated an energy of 235 ± 10 Mev. From these values an energy of 240 ± 10 Mev was assigned.

The energy spread of the main beam component was measured by experiments in which protons scattered from protons were deflected in the cyclotron field and detected in photographic plates.[9] An energy spread of less than 20 Mev at half maximum was indicated. Such energy definition is satisfactory if there are no appreciable components at lower energy. Such protons would distort the coincidence as a function of target position data (Figs. 3 and 4) because of the more nearly 90-degree angle between the protons and because of the increased effect of the magnetic field on the paths. Neither of these effects has been observed.

Production of low energy protons by cyclotron action with center well removed from the magnetic center was not appreciable. A target erected at 33-cm cyclotron radius reduced the counting level in our counters to a completely negligible amount.

The height of the beam was controlled by a clipper with 2.5-cm high opening and located about 250 degrees ahead of the target. Energy loss in multiple traversals that took place in the 12–72 mg/cm^2 polyethylene target were small. Small angle scattering was expected to remove protons from the beam after a few traversals. The measurements of energy spread by magnetic deflection involved targets of about this thickness with the same beam clipper in place.

Under typical conditions for this experiment, the cyclotron operated at 100 FM cycles per sec, providing beam pulses at the target of about 250 μ-seconds in length. Within this beam pulse, a fine structure was expected with a time between bursts of 5×10^{-7} sec due to the precession of the orbit. Because of this fine structure and of the underlying rf fine structure, there are only stepwise advantages as one decreases the resolving time of the coincidence circuit. We have tried on occasion a coincidence circuit with resolving time of 10^{-8} sec, but with poorer pulse-height discrimination, with not enough improvement in chance coincidences to warrant its use.

The level of cyclotron operation was very low: a typical beam current used was 10^{-12} ampere. Control of the cyclotron at this level was greatly facilitated by limiting its vertical starting aperture by adjustable curtains attached to the dummy dee.

Background

Because of the variation of beam structure with the target position, magnetic field, frequency modulation repetition rate, etc., it was necessary to observe the background rate under actual operating conditions of the experiment. This was done by moving the polyethylene target tangentially to the beam until no p-p coincidences were detectable, and there observing the background as a function of beam level. Two components appeared: a chance part which varied quadratically with the singles counting rate in one channel, and a part which varied linearly with the singles rate. The latter part was due to scattering from carbon in which two charged particles were emitted simultaneously with nearly the p-p angle between them. In either case, the background was evaluated by the above procedure and scattering data corrected accordingly. The carbon scattering was expected to be a slowly varying function of both scattering angle and angle included by the counters at the target. However, since this background depends on the product of the total solid angles of the two counters, there was an appreciable difference between the background on the large angle side of the coincidence peak as compared with the small angle side. The average between the values on either side was used in correcting for the background at the center of the coincidence peak, since data obtained with carbon targets showed an approximately linear variation. The carbon background was larger at large angles of scattering where one might expect relatively undistorted nucleon-nucleon collisions would occur in the carbon nucleus.

Run Procedure

For each scattering angle selected, the counters were placed at calculated positions. A trial target was intro-

[8] P. R. Bell and W. H. Jordan, Rev. Sci. Instr. **18**, 703 (1947).
[9] O. A. Towler and C. L. Oxley, Phys. Rev. **76**, 461 (1949).

duced and its proper position found by movement of the target and observation of coincidences (see Figs. 3 and 4). With the target in proper position, integral number-discrimination level data were compiled and the flatness of the resulting curve examined (Fig. 6 is an example). If the curve was flat enough so that total fall in the top section was 10 percent or less, the alignment of the crystal was considered satisfactory and the discriminator set at the value corresponding to half traversal. This provided solid angle definition as previously discussed. The procedure was then repeated for the other counter. By moving the target to positions off the p-p coincidence peak, the chance and carbon background rates were determined as linear functions of the product of the two singles rates and of the singles rate in one channel respectively. After these preliminaries, the target was either left in place over-night, so that the C^{11} activity decayed to negligible amounts, or a new target was inserted in the measured position.

The beam stopper at 33-cm cyclotron radius was raised in order that protons would not reach the scattering target until the cyclotron oscillator was stabilized. After stabilization, the beam stopping target was removed and data collected. A run lasted approximately ten minutes, during which time one thousand to five thousand coincidences were recorded. Counting rates in the singles channels ranged from three thousand to twenty thousand per minute. A record of the counts in each singles channel was made each minute so that by use of the singles counts as a measure of incident beam, the fraction of activity induced during a particular minute was known and the proper correction for decay of the activity could be made. Following the run, the target was removed from the cyclotron and its activity measured with a standard beta-counter. Data on the separate runs made are given in Table I.

Corrections

The data were corrected, as noted before, for the background of chance and carbon coincidences. The decay of activity in the target was also considered. One further correction was necessary because of a characteristic of the discriminator circuit. The univibrator, which furnished the standard discriminator output pulse, had a dead time of two microseconds. As a result, true coincidences could be lost by the action of a prior single pulse in either channel. This loss has been calculated by considering the measured dead times, the length of beam pulse per FM cycle, the number of FM cycles per second, and the counting rates observed in each channel. The resulting corrections are listed in Table I. At most, they amount to 2.6 percent.

Beta-Calibration

A standard beta-counter was set up in a location remote from the cyclotron and provided with a massive lead shield to reduce background. The G-M counter used was an Amperex type 120c which had an end on mica window of 5.6 mg/cm^2 surface density and 4.9 cm diameter. The use of halogen quenching gas in these counters provides a long life. The inside of the lead shield was lined with methyl methacrylate plastic to reduce scattering. Target holders and shelves were provided so that the target could be accurately positioned before the counter. Because of the low level of activity in the targets, the counting was done with the sample 7 mm from the counter. With this small separation, centering and distribution of the activity had an appreciable effect on the efficiency of collection. This distribution was determined by covering the target with a series of plastic sheets in which were cut a circular opening and successive annular spaces, so that the relative activity at various distances from the center could be determined. A correction of less than 4 percent was computed by use of this information, and the measured variation in efficiency with distance from the center.

The counter operated from a regulated power supply and was used with either the Neher-Pickering preamp circuit, or with a quenching circuit[10] which imposed an artificial dead time of 600 μsec.

C^{11} is a positron emitter with an allowed energy spectrum ending at 0.95 Mev.[11] Calibration of the over-all efficiency of the counter for this radiation proceeded by three independent methods.

First, a calibration was obtained by use of a secondary radium E standard used by Aamodt, Peterson, and Phillips[6] in the calibration of the beta-counter used in measurement of the $C^{12}(p,pn)C^{11}$ cross section. The corrections required for different absorption in the counter arrangements were small. From the source strength, as given in terms of the equivalent Na^{24} activity, we obtained an over-all efficiency of 0.133 $\pm$0.009 for our counter when measuring the C^{11} positrons from a 12 mg/cm^2 source.

In the second method, the strength of C^{11} sources of about three millicuries were measured in a counting arrangement with geometrically determined efficiency. After several half-lives, these sources were counted in a lower shelf of the standard beta-counting apparatus. From this measurement, the known half-life, and comparison measurements of the efficiencies of the several shelves, a calibration of the efficiency at the shelf position used for the scattering targets was obtained. The auxiliary counting arrangement was a replica in important respects of that described by Curtiss and Brown.[12] Because of the considerable background from annihilation radiation, a shutter over the aperture was used to replace the shutter near the source. The baffle system was unchanged. Alcohol-argon counters were

[10] Cook-Yarborough, Florida, and Davey, J. Sci. Instr. **26**, 124 (1949).

[11] *Nuclear Data*, National Bureau of Standards Circular 499 (1950).

[12] L. F. Curtiss and B. W. Brown, J. Research Natl. Bur. Standards **37**, 91 (1946).

TABLE I. Data from individual runs.

C.m. angle, degrees	Observed coincidences	Background coincidences	Lost coincidences	C^{11} atoms produced	Solid angle	Lab cross section	C.m. cross section	R.m.s. statistical accuracy
						Millibarns per steradian		Percent
90	7976	590	179	1083×10^4	12.04×10^{-4}	14.07	4.81	1.2
79	2389	158	37	394	8.57	16.45	5.08	2.2
79	2058	132	27	343	8.57	16.28	5.02	2.0
70	2308	182	41	423	6.85	18.29	5.25	2.2
69.1	4681	394	124	941	6.71	17.11	4.87	1.6
69.1	4520	391	117	841	6.71	18.42	5.25	1.6
69.1	2829	197	55	558	6.71	17.56	5.00	2.0
49.2	1687	79	18	563	3.84	18.74	4.71	2.6
49.2	2083	72	26	674	3.84	19.61	4.93	2.3
48.6	891	31	14	315	3.58	19.77	4.96	3.5
48.6	1024	28	12	366	3.58	19.60	4.91	3.2
39.4	1698	135	28	786	2.37	21.34	5.14	2.6
39.4	1538	141	31	732	2.37	20.51	4.93	2.8
27.5	1103	53	13	876	1.412	21.05	4.86	3.2
27.5	1420	137	35	1098	1.412	20.82	4.81	2.9
26.8	767	88	16	632	1.348	19.96	4.60	4.0
26.8	619	55	11	486	1.348	21.44	4.94	4.3
26.8	1006	74	16	790	1.348	21.80	5.02	3.4

used (Tracerlab TGC-1). An efficiency of 0.125 ± 0.010 was measured.

The third used beta-gamma coincidence measurements made with Au^{198}. For this an additional gamma-counter of the same type was installed in the standard beta-counter housing. It was covered with a lead radiator and a plastic cover to minimize back scattering. The output pulses from the quenching circuits were fed to a conventional coincidence circuit with resolving time of 1.5 μsec. The Au^{198}, in foil irradiated by neutrons at the Oak Ridge National Laboratory, was evaporated to a thickness of about 100A on a collodion foil of approximately 100 $\mu g/cm^2$. Gold is a negatron emitter with allowed spectrum ending at 0.96 Mev, followed by a 0.411-Mev γ-ray.[11] Pile irradiated gold contains some Au^{199} produced in a secondary reaction. A measurement of the half-life of the sample indicated that the amount of Au^{199} present was small enough to be neglected. Counter behavior is critical, spurious counts and pulse delays due to attachment being possible sources of error. The artificial dead time imposition should remove spurious counts which generally occur with counter recovery. Coincidences from cosmic rays were measured as a function of delay between the two counters. The maximum delay measured 4 μsec. A correction of 12 percent was applied to the measured coincidences to compensate for those lost in this manner.

An efficiency of 0.138 ± 0.008 was measured by this method giving 0.132 ± 0.005 for the combined results of the three methods of measurement.

Target Composition and Recoil Losses

The polyethylene target material has a theoretical composition of $(CH_2)_n$. An analysis of a sample polyethylene sheet used was made by Paulson and Wichers at the National Bureau of Standards. Since their analysis agrees with that expected for a 2:1 hydrogen to carbon ratio within its 0.2 percent accuracy, the ratio of 2:1 has been used in calculating the cross sections.

An upper limit on the loss of C^{11} atoms from the target by recoil has been set by measuring the additional activity picked up in a 1.6 mg/cm^2 aluminum catcher foil surrounding a target of the minimum thickness used in scattering measurements. This activity amounted to $1.2^{+0.3}_{-0.6}$ percent. Return of recoil C^{11} ions to the target by the magnetic field was expected to reduce this loss considerably. No correction to the data has been applied for this loss.

EXPERIMENTAL RESULTS

Cross Sections

Table I presents the pertinent data collected in each run, coincidence corrections, solid angles, and differential cross sections calculated from the data. The absolute values were computed from the cross section of $49(\pm3)$ millibarns given by Aamodt, Peterson and Phillips[6] for the $C^{12}(p,pn)C^{11}$ process at 240 Mev.

Figure 7 presents the data graphically. Data from runs at substantially the same angle were combined in weighted averages. The errors shown at each angle include all estimated errors except those associated with the over-all absolute scale.

It will be noticed that the cross sections do not indicate any significant deviation from isotropic scattering in the angular range studied. Assuming isotropic scattering, a weighted average cross section for all angles has significance. It has been determined as 4.97 millibarns/sterad. with an associated absolute error of 0.43 mb/sterad. The figure indicates this value and assigned error.

Accuracy of Cross Sections

In addition to statistical errors, other errors have been considered and their magnitudes estimated. Sources of

error include geometrical errors, pulse-height selection errors, correction uncertainties in background and losts counts, beta-counting errors, errors due to loss of activated carbon, and the uncertainty in the carbon cross section. These errors have been considered so as to assign an uncertainty to the absolute scale and, in addition, to the separate measurements. The uncertainties independent of the absolute scale have been indicated in Fig. 7. These range from 3.5 to 5.5 percent and are chiefly the result of geometrical effects and statistics. The absolute scale error is 8.4 percent, and arises mostly from the beta-calibration error and carbon cross section uncertainty.

Examination of the internal consistency, as may be done by reference to Table I, shows deviations in the various runs as might be expected from the statistical uncertainty plus small additional errors assigned.

DISCUSSION

Comparison with Other Experimental Data

Figure 7 includes the data obtained at 250 Mev by Chamberlain, Segrè, and Wiegand.[2] Errors indicated are on the same basis as ours. Although there is no disagreement in the angular distribution in the overlapping range, the difference in absolute values is unduly large, amounting to 29 percent. The errors assigned by the two groups of experimenters are 8.8 percent (Berkley) and 8.6 percent (Rochester). The wide divergence points to an unnoticed systematic error either in these or allied experiments. The Berkley experiment is more direct in its calibration of the beam measuring instrument. This was a thin argon filled ionization chamber which was compared with a Faraday cage at 345 Mev and its sensitivity calculated at 250 Mev from well established semi-empirical relations.

As described previously, our current measurement relies on the absolute calibration of our beta-counter and the value of the $C^{12}(p,pn)C^{11}$ cross section at 240 Mev. This cross section was determined by Aamodt, Peterson, and Phillips[6] by direct use of a Faraday cup. Our use of a RaE secondary standard calibrated by Aamodt *et al.*, reduces the possibility of a systematic difference in beta-calibrations.

It may be noted that the measurements of Birge, Kruse, and Ramsey[3] at 75 and 105 Mev, made in the same manner as ours, indicate an almost identical discrepancy with the Berkley measurements at 120 Mev if it is assumed that there is no unusual drop in the cross section between 105 and 120 Mev.

These discrepancies indicate that further independent absolute measurements of the carbon or *p-p* cross section would be valuable in the range from 100 to 250 Mev. Some preliminary results of a measurement of the *p-p* cross sections, using carbon as a detector of the scattering as well as a monitor of the incident beam, are in agreement with the 4.97 mb/sterad value of the cross section.

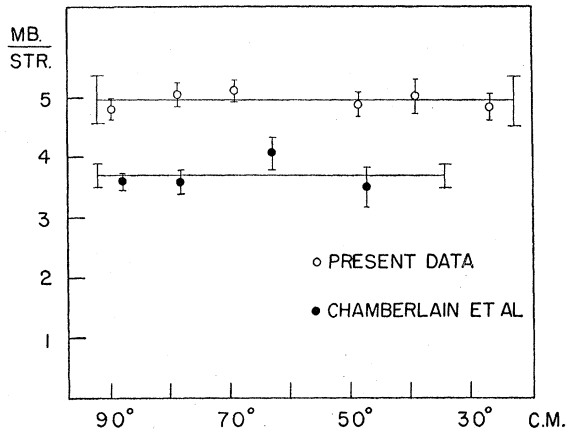

FIG. 7. Differential c.m. cross sections.

Comparison with Theory

The present results offer little new for theoretical interpretation except for the extension of the known isotropic behavior to 27 degrees at this energy. The lack of agreement of the absolute cross section with other data at this energy makes the data of no present use in regard to the energy dependence of the cross section.

Early results of this experiment, which indicated a cross section of 8^{+8}_{-4} mb/sterad at 90 degrees, showed that the *n-p* interaction of Christian and Hart[13] could not be used directly for the *p-p* interaction since it predicted a cross section too small by a factor over ten. Since then, several theoretical approaches have been made, particularly with the purpose of fitting the data of Panofsky *et al.*[14] and Cork *et al.*[15] at 30 Mev, and of Chamberlain *et al.*[2] at 345 Mev. These include that of Christian and Noyes,[16] in which an additional *p-p* tensor interaction is used to fit the data, and those of Case and Pais[17] and Jastrow[18] which retain the equality of *n-p* and *p-p* forces in the same states, and fit the *p-p* data by use of $(\mathbf{L}\cdot\mathbf{S})$ coupling and a repulsive singlet core, respectively. Further extensions of the angular range of high energy scattering measurements to include Coulomb interference effects, polarized scattering measurements, and, perhaps, *p-d* scattering data, may aid in deciding on the proper interaction.

We wish to thank Professor S. W. Barnes for his continued interest and support of this work. We are also indebted to the mechanical engineering staff and the operating crew of the cyclotron.

[13] R. S. Christian and E. W. Hart, Phys. Rev. **77**, 441 (1950).
[14] W. K. Panosky and F. L. Filmore, Phys. Rev. **79**, 57 (1950).
[15] Cork, Johnson, and Richman, Phys. Rev. **79**, 71 (1950).
[16] R. S. Christian and H. P. Noyes, Phys. Rev. **79**, 85 (1950).
[17] K. M. Case and A. Pais, Phys. Rev. **80**, 203 (1950).
[18] R. Jastrow, Phys. Rev. **81**, 165 (1951).

Note added in proof: Cassels, Staford, and Pickavance have reported *p-p* scattering at 146 Mev [Nature **168**, 468 (1951)]. This data based on the C^{11} cross section together with latter results [private communication] based on photographic measurement of the incident beam give a combined result of 4.86 ± 0.25 mb/sterad. This is higher than that of Chamberlain *et al.* by the same amount as ours.

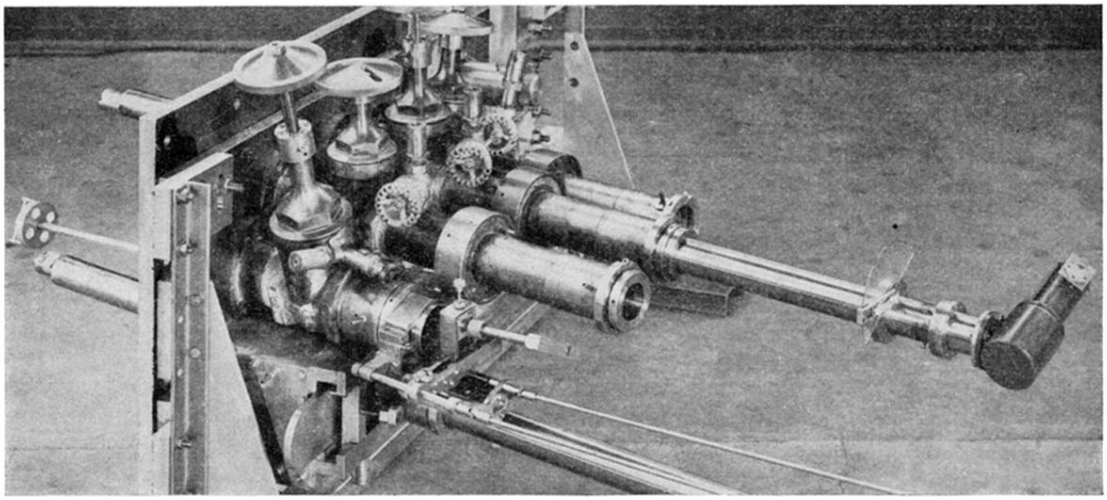

FIG. 2. Photograph of scattering apparatus on cyclotron port plate.